Journal of Macromolecular Science, Part A
Publication details, including instructions for authors and subscription information:
http://www.informaworld.com/smpp/title~content=t713597274

Synthesis, Characterization, Curing and Shape Memory Properties of Epoxy-Polyether System

J. Dyana Merline[a]; C. P. Reghunadhan Nair[a]; K. N. Ninan[a]
[a] Propellants and Special Chemicals Group, PCM Entity, Vikram Sarabhai Space Center, Thiruvananthapuram, India

To cite this Article Merline, J. Dyana , Nair, C. P. Reghunadhan and Ninan, K. N.(2008) 'Synthesis, Characterization, Curing and Shape Memory Properties of Epoxy-Polyether System', Journal of Macromolecular Science, Part A, 45: 4, 312 — 322
To link to this Article: DOI: 10.1080/10601320701864245
URL: http://dx.doi.org/10.1080/10601320701864245

Journal of Macromolecular Science®, Part A: Pure and Applied Chemistry (2008) **45**, 312–322

ISSN: 1060-1325 print/1520-5738 online
DOI: 10.1080/10601320701864245

Synthesis, Characterization, Curing and Shape Memory Properties of Epoxy-Polyether System

J. DYANA MERLINE, C. P. REGHUNADHAN NAIR, and K. N. NINAN

Propellants and Special Chemicals Group, PCM Entity, Vikram Sarabhai Space Center, Thiruvananthapuram, India

Received August, 2007, Accepted September, 2007

Epoxy resins were cured by an amine telechelic poly(tetramethylene oxide) (PTMO). The telechelic amine was synthesized from hydroxy telechelic PTMO and was characterized. The kinetics of curing of epoxy monomer by the polyether amine was studied in detail by differential scanning calorimetry (DSC) and rheology to optimize the cure conditions. The cured epoxy system exhibited shape memory properties where PTMO served as the switching segment. Molar ratios of the epoxy monomer and the amine were varied to get polymers with different compositions. The developed polymers were analyzed by DSC, X-ray diffraction, and Dynamic Mechanical Thermal (DMTA) analyses. Shape memory property was evaluated by bending tests. As the concentration of epoxy resin increased, the transition temperature (T_{trans}) increased. The tensile strength and % elongation also increased with epoxy resin-content. The extent of shape recovery increased with PTMO-content with a minor penalty in recovery time. The polymer with the maximum PTMO-content exhibited 99% shape recovery with a recovering time of 12 s.

Keywords: shape memory polymer; epoxy resin; poly(tetramethylene oxide); cure kinetics

1 Introduction

Shape memory materials have received increasing attention in recent years owing to their interesting properties and many potential applications. The shape memory effect in materials is essentially the capacity to recover mechanically induced and "frozen" strain upon application of heat, magnetic field, or electric field (1–4). The change in shape induced by changing temperature is known as a thermally induced shape memory effect. It can be achieved by changing the operation temperature to below or above the switching transition temperature (T_{trans}). Normally, the transition temperature corresponds to either a glass transition (T_g) or the melting (T_m) of the polymer. Shape memory polymers (SMP) generally consist of two components, crosslinks to determine the permanent shape and the switching segments with a definite T_{trans} to fix the temporary shape (4, 5). Above $T_{trans,}$ the permanent shape can be deformed by application of an external stress. On cooling below T_{trans} and unloading the external stress, the temporary shape can be fixed. The polymer recovers the permanent shape on heating above T_{trans} (6–12). SMP materials have the ability to recover large strains imposed by mechanical loading. They are designed to have a large change in elastic modulus above and below the transition temperature (13). A large difference in elastic modulus leads to better and faster shape recovery properties. The driving force for the shape memory recovery property is the elastic strain generated during deformation (14).

Excellent shape memory effects have often been observed with block or segmented copolymers (15–20). Among the various SMPs, polyurethanes are the most popular (21–23). Elastic Memory Composites (EMC), the composites derived from shape memory resin are a newly developed class of materials hosting an ideal combination of properties for deployable space structures. EMC materials retain the structural properties of traditional fiber-reinforced composites, while also functioning as shape memory materials. These properties enable the creation of structurally efficient, controllable, deployable space structures and deployment mechanisms with no moving parts. Though PU shows good shape memory properties, they are not very good matrices for reinforced composites. Use of epoxy resin-based systems in shape recovery EMC is of great interest due to the ease of processibility of epoxy matrix and the strength characteristics of its composites. Several studies on EMC for deployable devices have been reported. They made use of epoxy resin-based (24, 25) or cyanate ester resin-based (26) shape

Address correspondence to: C. P. Reghunadhan Nair, Propellants and Special Chemicals Group, PCM Entity, Vikram Sarabhai Space Center, Thiruvananthapuram 695022, India. Fax: +91-471-2706136; E-mail: cprnair@gmail.com

memory composites. However, the published articles focused mainly on device fabrication. The information on the synthesis and characterization of the resins responsible for the shape memory properties of the composites are often not disclosed. A good deployable composite system warrants synthesis of shape memory polymers with good processibility and excellent shape recovery characteristics. The published information in this respect is very scarce.

Here, we report the synthesis of epoxy resin-based SMP from an amine-terminated poly(tetramethylene oxide) and different epoxy resins. The synthesis, characterization, cure kinetics, mechanical properties and shape memory properties are described. The dependencies of these properties on the resin composition have been examined.

2 Experimental

2.1 Materials and Method

Hydroxy telechelic poly(tetramethylene oxide) (PTMO) (Aldrich, M_n 2000), Epoxy resin (GY-250, diglycidyl ether of bisphenol A with an epoxy value of 5.4 eq/kg, Ciba Geigy, India) EPN-1179 (Novalac epoxy, epoxy value-5.6 eq/kg, Ciba Geigy, India), triphenylolmethane triglycidylether (TRI, epoxy value-5.6 eq/kg, Aldrich Chemicals) tolylene diisocyanate (TDI, Aldrich Chemicals) and 4,4′-methylenedianiline (MDA, Aldrich Chemicals) were used to synthesize epoxy-based shape memory polymer. PTMO and epoxy resin were dried in flash evaporator for 5 h at 80°C before use. AR grade ethyl methyl ketone (MEK, SRL India) was used as solvent. TDI and MDA were used as received.

2.2 Polymer Synthesis

2.2.1 Synthesis of Amine Terminated PTMO

A 500 ml round bottomed, three-neck flask equipped with a mechanical stirrer, nitrogen inlet and condenser with drying tube was charged with TDI (10.44 g). N_2 gas was bubbled through TDI at 60°C. To this, a calculated amount of PTMO (40 g PTMO in 93.3 g MEK) was added drop wise and the reaction mixture was stirred under N_2 at 65°C for 2 h to make the isocyanate terminated prepolymer. To a solution of MDA (47.5 g) in 190 g MEK, the isocyanate-terminated prepolymer was added drop wise at room temperature under mechanical stirring to get the amine-terminated PTMO. The resulting solution was filtered through a G-3 grade sintered crucible. The filtrate was then concentrated in a flash evaporator and added drop wise to methanol to precipitate the product. The precipitate was then washed with methanol to remove the impurities present. It was then dried in vacuum at 65°C/2 h. The amine-terminated PTMO was characterized by FTIR and chemical analyses.

2.2.2 Amine: Epoxy Cure Reaction

Amine-terminated PTMO was then mixed with epoxy monomer in the required ratio by dissolving both in MEK (70% by wt) at room temperature. The mixture was then evacuated and poured on to Teflon sheets. The cure reaction was carried out by heating the system slowly to its cure temperature (cure temperature was determined from DSC and rheological studies, which will be discussed later) and maintaining it at this temperature for 3 h.

2.3 Characterization

2.3.1 DSC Analysis

DSC analysis was performed in a Mettler DSC-20 analyzer for cure characterization of different epoxy resin-amine systems. A 1:1 stochiometric ratio of epoxy resin and amine was used for the cure characterization. For dynamic heating experiments, five different heating rates were employed; 2, 5, 7, 10, and 15°C/min from room temperature to 200°C. Fractional conversion vs. temperature data was obtained from this dynamic analysis from the system software. Thermal properties of the cured polymers were investigated by a DSC experiment. For this, the samples were heated from −50°C to 200°C at a heating rate of 5°C/min. The data of first run was used for the analyses.

2.3.2 Physical, Chemical and Spectroscopic Analyses

FTIR studies were performed using a Perkin-Elmer GX-A model FTIR spectrophotometer using ATR (attenuated total reflectance) accessory with diamond crystal. Spectrum was recorded in the range of 4000 to 550 cm^{-1} with a resolution of 4 cm^1. Chemical analysis was performed to find out the amine value from which, the molecular weight of the synthesized precursor polymer was assessed.

2.3.3 Rheological Analysis

Reological characterization was done with a Reologica Stresstech Rheometer model Reologica Viscotech QC using a 20 mm parallel plate assembly in oscillation mode at a frequency of 1 Hz and a controlled strain of 0.01. The epoxy resin-amine mixture was mixed thoroughly and loaded on the plate at 50°C. The gap between the plates was maintained at 0.5 mm. The data analysis was done with the instrumental software. Curing temperature and curing time were studied from this.

2.3.4 X-ray Diffraction Studies

X-ray scattering studies were performed in a 'X' Pertpro (P Analytical, Netherlands) using the filter Ni, the target as Cu Kα radiation (λ of 1.5405 A°) at 40 KV and 30 mA current. The diffraction patterns of the samples of thickness 1 mm were recorded for Bragg's angle, 2Θ from 0 to 40°.

2.3.5 Mechanical Tests

Mechanical properties were determined with a tensile tester (UTM 4469). The micro tensile test specimens had the dimensions of 75 mm × 5 mm × 1 mm as per ASTM D 412. The gauge length and crosshead speed were 33 mm and

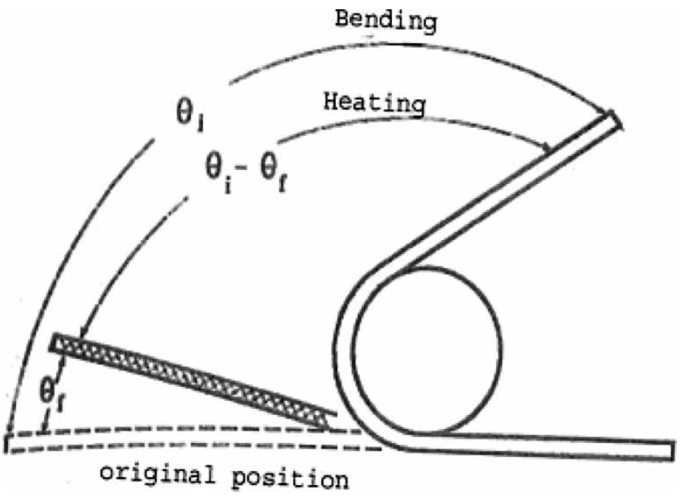

Fig. 1. Schematic representation of bending test for shape memory tests.

200 mm/min, respectively. At least three specimens were tested, and the average of the measured property was taken.

2.3.6 *Dynamic Mechanical Thermal Analysis*

Dynamic mechanical properties were determined in a Rheometrics Scientific Model Mark IV (UK) analyzer in the tensile mode at a frequency of 1 Hz.The specimens were heated from -150°C to 150°C at a heating rate of 5°C/min. The data of storage modulus and tan δ were recorded.

2.3.7 *Shape Memory Evaluation*

The method of evaluating shape memory alloy as reported by Lin and Chen (27) was adopted for the polymers, as shown in Figure 1. A straight rectangular strip of the polymer of dimension 100 mm × 10 mm × 2 mm was used for the tests. The polymer was heated to a temperature T_{trans} $+20^{\circ}$C and deformed to an angle (θ_i) (90°) and then cooled to a temperature T_{trans} -20°C to fix the deformation. Then, the deformed polymer was heated to T_{trans} $+20^{\circ}$C, and the change in angle (θ_f) was recorded. The ratio of recovery was found as $(\theta_i - \theta_f)/\theta_i$. Each time, the samples were subjected to five bending tests and the value of the fifth attempt was taken.

3 Results and Discussion

3.1 *Synthesis and Formulations*

A two-step process, as per Scheme 1, was chosen for the synthesis of amine-cured epoxy shape memory polymer. In the first step, OH-terminated PTMO was reacted with tolylene diisocyanate to get -NCO terminated PTMO. The -NCO terminated PTMO was then used for deriving the amine terminated PTMO by reaction with excess methylene dianiline (MDA). The amine-terminated PTMO (amine-PTMO) was characterized by FTIR and chemical analyses. Figure 2 shows the FTIR spectrum of amine-PTMO. The spectrum shows the absence of -NCO peak at 2200 cm^{-1} and the presence of -NH_2 peak at 3300 cm^{-1} indicating the formation of amine terminated-PTMO. The peak at 1710 cm^{-1} and 1620 cm^{-1} correspond to the -C═O absorptions of urethane and urea groups respectively. From chemical analysis (28) (by amine value determination), the average molecular weight of synthesized amine-PTMO was found to be 2200 g/mol. The amine-PTMO was then reacted with epoxy monomer in varying stochiometry to get amine-PTMO-cured epoxy polymer.

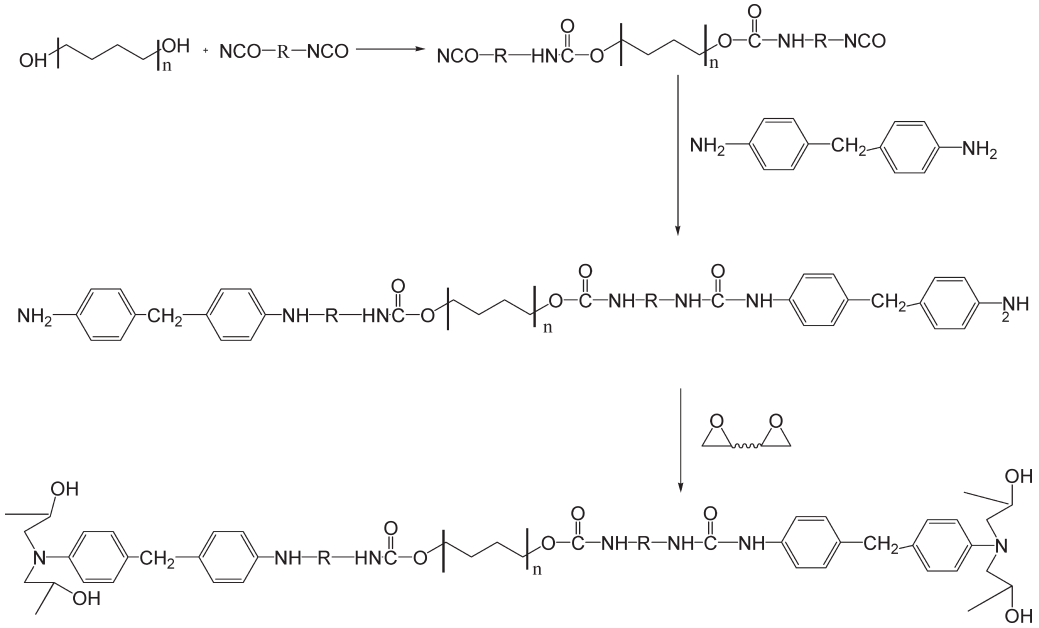

Sch. 1. Synthetic route for amine-epoxy polymer.

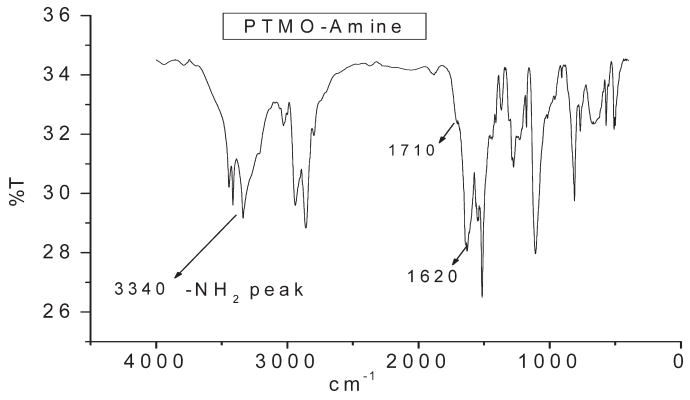

Fig. 2. FTIR spectrum of amine terminated PTMO.

Table 1 compiles the formulations for the amine-cured epoxy polymer. The hard segment content constituted by the epoxy resin, urethane and urea segments was varied from 54 to 82 weight percentages. For GY epoxy resin series, with an increase in hard segment-content, the transition temperature (T_{trans}) also increased. This implies the increased rigid nature of the polymer system due to the generation of a higher number of crosslinks. With the EPN system, a transition temperature of 77°C and with TRI system, T_{trans} of 110°C were observed for a 1:1 stochiometry of amine and epoxy resin. Comparing the three different epoxy systems (GY-1.0, EPN-1.0, and TRI-1.0) with the same amine: epoxy (1:1) equivalents, lowest T_{trans} was observed for the EPN system. Here, each -NH_2 group corresponded to two epoxy groups.

3.2 Rheological Cure Characterization of Polymers

Rheological cure characterization was carried out for the three different epoxy-based systems (GY-1.0, EPN-1.0, TRI-1.0) of amine-epoxy resin stochiometry of unity. To study the cure temperature, storage shear modulus (G′) of the three different epoxy systems was monitored as a function of temperature (T). Figure 3 shows the variation of G′ with temperature for GY-1.0, EPN-1.0, and TRI-1.0. The gelation sets in at lower temperature for the TRI and EPN systems. The diepoxy system needs a higher temperature. The absolute modulus at the end of cure (stagnating modulus) was inversely proportional to the functionality of epoxy monomer. Maximum G′ modulus was observed for GY-1.0 with an epoxy group functionality of 2. Curing temperature (T_{max}) was taken as the midpoint of the G′ vs. temperature graph and it was found to be 140°C, 135°C, and 130°C for GY-1.0, EPN-1.0, and TRI-1.0, respectively. Isothermal rheological analyses were done at the T_{max} to optimize the curing time. The corresponding data are shown in Figure 4. The isothermal profiles show the relative trend in modulus for the three different epoxy systems.

A few minutes curing at T_{max} is adequate to bring about the cure completion. The duration for cure completion was observed as 18, 15, and 20 min for GY-1.0, EPN-1.0, and TRI-1.0 epoxy systems at their respective T_{max}. Based on these studies, the cure temperature and cure time were optimized for each system.

Rheological fractional conversion at any time was calculated using Equation (1):

$$\alpha = \frac{G'(t)}{G'(\infty)} \tag{1}$$

Where, G′(t) is the storage modulus at time 't' and G′(∝) is the maximum storage modulus (stagnating modulus) at each temperature. Figure 5 shows the time-conversion plot generated from rheological analysis at the cure temperature. For the three different epoxy systems, fractional conversion showed a rapid increase with time. From the isothermal conversion, it is observed that the reaction is completed in about 10 min for all the three different epoxy systems. The completion of reaction was also confirmed by FTIR and DSC analysis, which is discussed later.

3.3 DSC Analysis

DSC analysis was performed to determine the cure kinetics, as well as thermal properties of the cured polymer systems. To study the cure kinetics, DSC analysis was carried out for the three different amine-epoxy resin systems (GY-1.0, EPN-1.0 and TRI-1.0) using the same amine-epoxy equivalent ratio, at variable heating rates (2, 5, 7, 10 and 15°C/min).

In Table 2, the cure maximum (T_{max}) obtained from the DSC curve for the three different epoxy systems at different heating rates is compiled. With an increase in heating rate,

Table 1. Formulations of epoxy-based SMP

Sample	Type of epoxy resin	Equivalent ratio of amine:epoxy	% Hard segment	T_{trans} (°C) (taken from DMA)
GY-0.8	GY-250	1:0.8	74	83
GY-0.9	GY-250	1:0.9	77	95
GY-1.0	GY-250	1:1	79	96
GY-1.1	GY-250	1:1.1	82	110
EPN-1.0	EPN-1179	1:1	54	77
TRI-1.0	Triphenylolmethane triglycidylether (TRI)	1:1	54	110

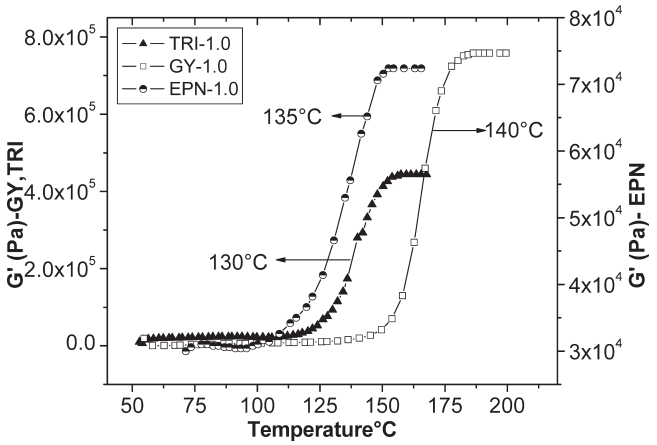

Fig. 3. Variation of G′ with temperature for three epoxies at 1:1 amine:epoxy equivalent ratio.

T_{max} also increases. Though the absolute values are different, the trends in T_{max} for the three systems are identical in both DSC and rheological analysis (ie GY > EPN > TRI).

3.3.1 *Cure kinetics*

For the determination of reaction order of epoxy: amine reaction, Coats-Redfern (C-R) method (29) was adopted. The C-R Eq. (2) is:

$$\ln\left[\frac{g(\alpha)}{T^2}\right] = \ln\left[\left(\frac{AR}{\beta E}\right)\left(1-\frac{2RT}{E}\right)\right] - \frac{E}{RT} \qquad (2)$$

where α is the fractional conversion at temperature T, β is the heating rate, E is the activation energy for cure, A is pre-exponential factor and R is the gas constant.

Where,

$$g(\alpha) = \left[1 - \frac{(1-\alpha)^{1-n}}{1-n}\right] \quad \text{for } n \neq 1$$

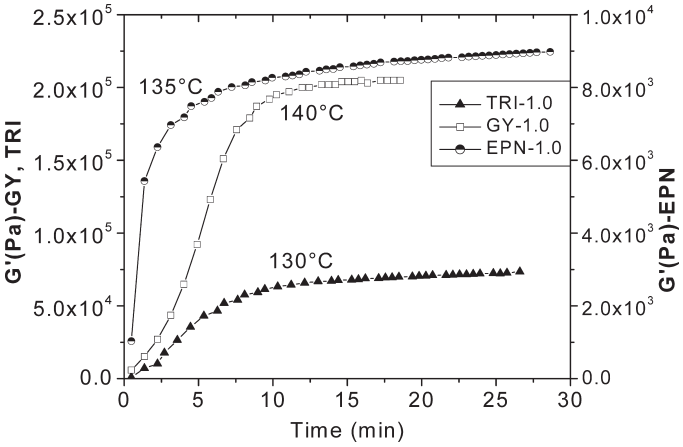

Fig. 4. Variation of G′ with time at cure temperature for three amine-epoxy systems (140°C for GY-1.0, 135°C for EPN-1.0 and 130°C for TRI-1.0).

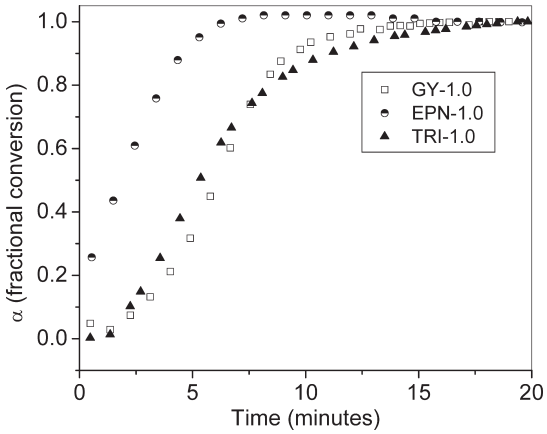

Fig. 5. Time-conversion profiles (from rheology) for the three amine–epoxy resin systems at cure temperatures, 140°C for GY-1.0, 135°C for EPN-1.0 and 130°C for TRI-1.0.

and

$$g(\alpha) = -\ln(1-\alpha) \quad \text{for } n = 1$$

The conversion at any temperature α_T, was found from the relation:

$$\alpha_T = \frac{\Delta H_f}{\Delta H_T}$$

where, ΔH_f is the fractional enthalpy at that temperature and ΔH_T, the total heat of reaction. ΔH_f and ΔH_T were obtained from the fractional and total areas under the exothermic curve in DSC. For determining the order, the α data for an amine-epoxy resin mixture in 1:1 equivalent ratio were used. The reaction order was found from the best fit of the linear plot of $\ln[g(\alpha)/T^2]$ against $1/T$ for different assumed values of n as per Equation (2). A typical C-R plot is shown in Figure 6 for the cases of n = 0.5, 1, 1.5, 2, and 2.5, respectively. The best linear fit was obtained for n = 1. Thus, the order of the reaction was taken as one. Similar observation was made for EPN and TRI systems. A reaction order of one has been reported for several epoxy resin-amine systems, investigated by the DSC technique.

3.3.2 *Ozawa and Kissinger Method*

The activation parameters were calculated by the Ozawa (30–32) and Kissinger (33), methods that is based on a variable program rate. The Ozawa method uses a plot of the logarithm of the heating rate vs. the reciprocal of peak temperature, which gives a straight line. Using the slope of the line, activation energy can be calculated using the following Equation (3):

$$E \cong 2.15R\,\frac{d(\log\beta)}{d(1/T)} \qquad (3)$$

where E is the activation energy, R is gas constant, β is the heating rate in °C/min and T is the peak temperature in the Kelvin scale.

Table 2. T_{max} from DSC analysis at variable heating rates

Sl. no.	System	T_{max} from DSC at different heating rate (°C)				
		2 (°C/min)	5 (°C/min)	7 (°C/min)	10 (°C/min)	15 (°C/min)
1	GY-1.0	103	125	128	134	137
2	EPN-1.0	88	115	118	120	127
3	TRI-1.0	82	107	109	115	124

The E values calculated for the three different amine-epoxy resin systems are included in Table 2. Maximum activation energy of 61.7 kJ/mol was observed for the GY system. A representative Ozawa plot can be found in Figure 7.

An alternative method for the calculation of activation energy is according to the Kissinger method. It is based on a plot of $\ln(\beta/T^2)$ vs. $1/T$ which gives a straight line. From the slope of the line, E can be calculated as per the following Equation (4):

$$\frac{d\ln(\beta/T^2)}{d(1/T)} = -E/R \tag{4}$$

The related Kissinger plot is shown in Figure 8. The E values calculated for the three different epoxy systems are given in Table 3. The maximum activation energy was again observed for the GY system. The E values by the two methods are effectively identical.

The pre-exponential factor A was calculated in both methods by the following Equation (5):

$$A = \beta\left(\frac{E}{RT^2}\right)e^{E/RT} \tag{5}$$

The average value of A as calculated from different heating rates are included in Table 3.

The rate constant k at a given temperature was calculated using the Equation (6):

$$k = Ae^{-E/RT} \tag{6}$$

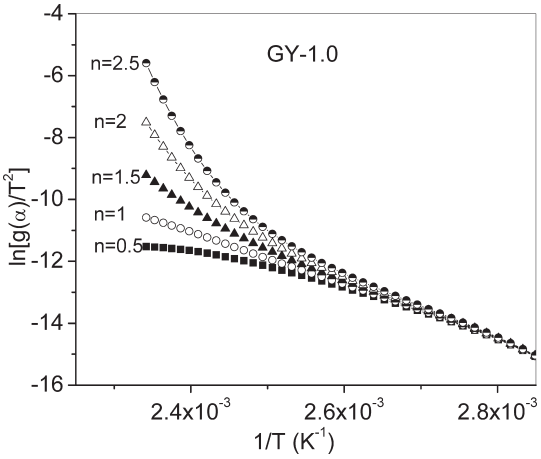

Fig. 6. C-R plot of determining the order of reaction for the amine-epoxy resin reaction.

Where A is the pre-exponential factor, E is the activation energy, R is the gas constant and T is temperature in Kelvin scale. The k values at respective T_{max} values (from rheological analysis) are included in Table 3. Though the activation energies are different for the three different epoxy resins, there is a proportional change in the pre-exponential factor (A). The rate constants calculated at T_{max} are more or less the same for all the three systems.

3.3.3 *Kinetic Prediction of Isothermal Cure*

E and A are useful for the prediction of isothermal conversion. For the first order reaction, the relation for fractional conversion (α) and time (t) is given by Equation (7):

$$-\ln(1-\alpha) = kt \tag{7}$$

where $k = A\, e^{-E/RT}$

Figure 9 shows the predicted α vs. time plot for three different epoxies at their respective T_{max}. It shows that the cure is practically completed within 10 min for all the three different epoxies. It can be seen that both the theoretical (from DSC) and the experimental (from rheology) isothermal conversion profiles match each other. The kinetic data were useful for fixing the cure schedule of the polymers (detailed in the Experimental part). Though the reaction is complete in 10 min at the respective T_{max}, the polymers were maintained at this temperature for 180 min, to ensure the complete conversion.

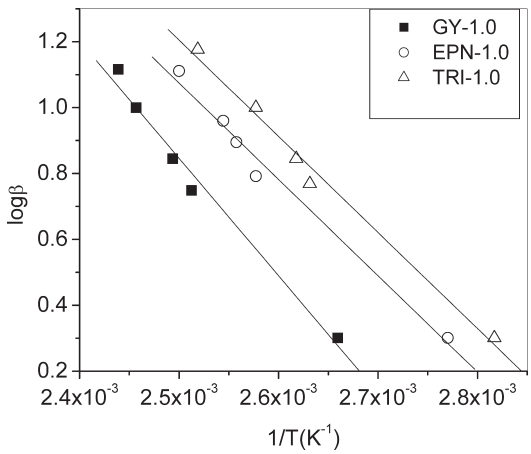

Fig. 7. Ozawa plot for the determination of E and A.

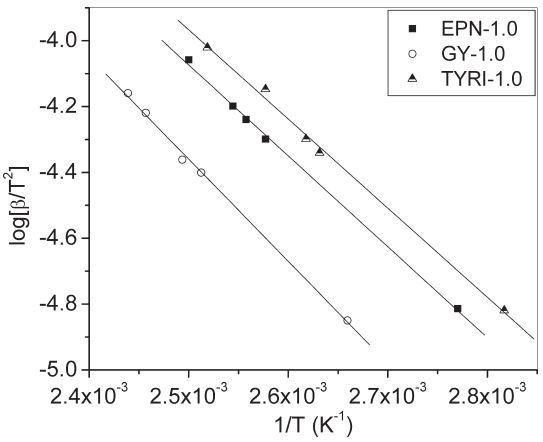

Fig. 8. Kissinger plot for the determination of E and A.

3.3.4 Thermal Characterization of Polymers

The amine:epoxy group equivalent ratio was varied from 1:0.8 to 1:1.1 in the case of GY. The DSC profiles of the cured polymers are shown in Figure 10. For the GY series, the crystal melting becomes more distinguished with an increase in PTMO content. GY-0.8 and GY-0.9 with more PTMO content exhibited melting endotherm at ~25°C corresponding to the crystal melting of PTMO. TRI-1.0 exhibited both crystallization and crystal melting temperatures at −30°C and 20°C, respectively. No definite crystallization or crystal melting could be observed in the DSC for the EPN system. No clear glass transition was observed in the DSC thermograms for the cured epoxy resins with the exception of the TRI system, which showed a glass transition at 53°C.

3.4 FTIR Analysis

FTIR analysis was carried out to find the completion of the reaction. Figure 11 shows the FTIR spectrum of epoxy system (GY-1.0) just after mixing and after curing. Cured sample (GY-1.0) showed the absence of absorption at 914 cm^{-1} due to epoxy groups and the presence of -OH absorption at 3400 cm^{-1}. This substantiates the ring-opening of epoxy groups. Interestingly, both the uncured and the cured samples exhibited a small sharp peak at ~2140 cm^{-1}. The spectrum of precursor amine-PTMO, shown in Figure 2 did not show any such absorption. Since the amine or the epoxy monomer does not show any such

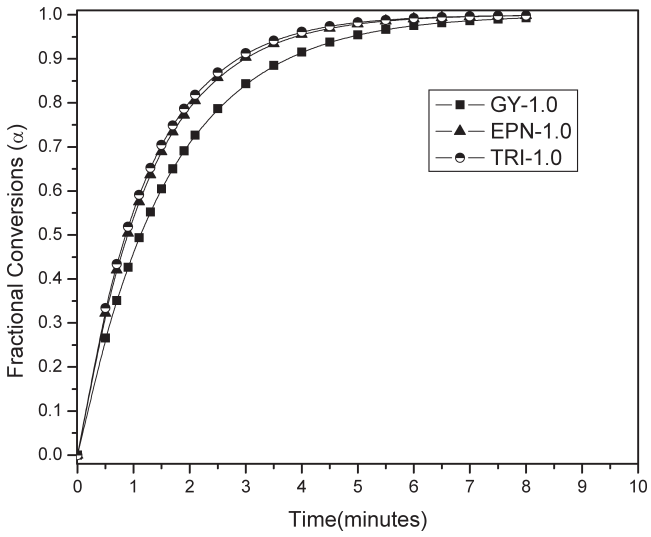

Fig. 9. Predicted conversion vs. time graph for the epoxy resin cure reaction at T_{max} in rheogram (140°C for GY-1.0, 135°C for EPN-1.0 and 130°C for TRI-1.0).

absorption, it was of interest to elucidate the origin of this peak in their mixture. It was doubtful that the urea linkage in the PTMO terminal could be contributing to the generation of groups, absorbing at ~2140 cm^{-1}. To confirm this, IR studies were carried out on the reaction products of diphenyl urea and a diepoxy monomer (GY-250) at 1:1 equivalent ratio. Figure 12 shows the FTIR spectra of the initial mixture of diphenyl urea and epoxy monomer at ambient condition.

FTIR spectrum shows a peak at 2144 cm^{-1}. One likely reason for the absorption at 2144 cm^{-1} is the formation of carbodiimide group -N═C═N- (34). In this case, a weak, broad absorption at ~3500 cm^{-1} indicates the generation of the OH group. The -NH-CO-NH- linkage in the amine-PTMO on reaction with epoxy groups could generate carbodiimide (-N═C═N-) groups, whose IR absorption occurs at ~2144 cm^{-1}. IR spectra of the individual components (diphenyl urea and GY-250) are shown in Figure 13. The spectra of these two components lack the IR absorption at ~2144 cm^{-1}. From this, it was confirmed that the origin of absorption peak ~2144 cm^{-1} is from the reaction between the urea group (present in PTMO terminal) and the epoxy group. It has been reported that N,N′-disubstituted urea can give rise to carbodiimide in the presence of dehydrating agents (34). Here, epoxy groups act as the dehydrating

Table 3. Kinetic parameters from DSC cure studies by different methods

	Ozawa			Kissinger		
System	E (kJ/mol)	A × 10^6 (min^{-1})	k at T_{max} (min^{-1})	E (kJ/mol)	A × 10^6 (min^{-1})	k at T_{max} (min^{-1})
GY-1.0	61.7	37	0.102	62.2	44	0.101
EPN-1.0	52.4	3.3	0.087	52.4	3.3	0.087
TRI-1.0	52.2	4.1	0.085	51.8	3.6	0.085

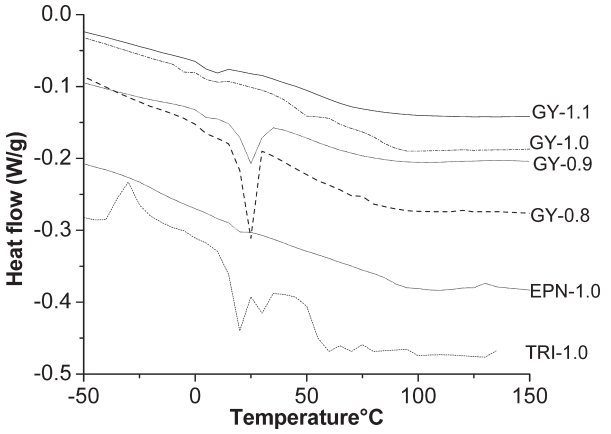

Fig. 10. DSC thermograms of polymers; Heating rate: 5°C/min (first heating).

agent (itself forming glycols). The proposed mechanism for the formation of carbodiimide group is shown in Scheme 2. This reaction generates OH groups whose absorption occurs at $\sim$3500 cm^{-1}. From the low intensity of these peaks, it is concluded that the carbodiimide group is formed only in smaller concentration and that it could not affect the polymer properties significantly. On curing of the resin, the peak at 2144 cm^{-1} becomes broadened and the peak maximum shifts to 2102 cm^{-1} (Figure 11).

3.5 X-ray Diffraction Analysis

Figure 14 shows the X-ray diffraction profiles of the cured resins. All the systems exhibited an identical XRD pattern. The diffraction profiles show a diffused diffraction maximum at $2\theta = 20^{\circ}$, suggesting the absence of defined PTMO crystallites at the test temperature. Since the crystallization and crystal melting were observed in DSC, it is obvious that the polymer can possess crystallites. The possible reason for the broad diffraction is that the XRD analyses were done at a temperature of 25°C, which is close to the crystal melting temperature of PTMO. In order to confirm this, XRD was

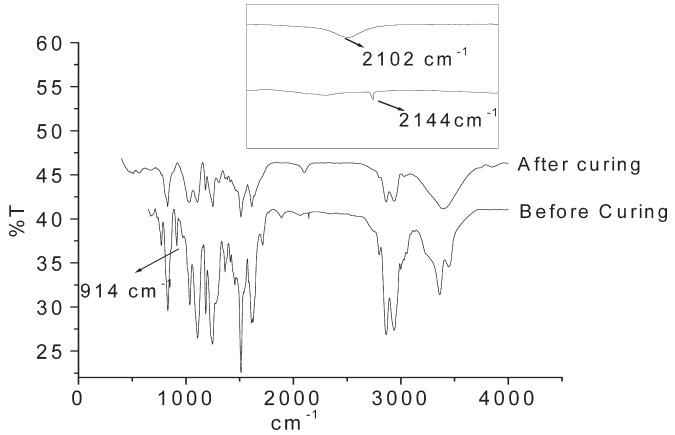

Fig. 11. FTIR analysis of the sample, GY-1.0 immediately after mixing and after curing.

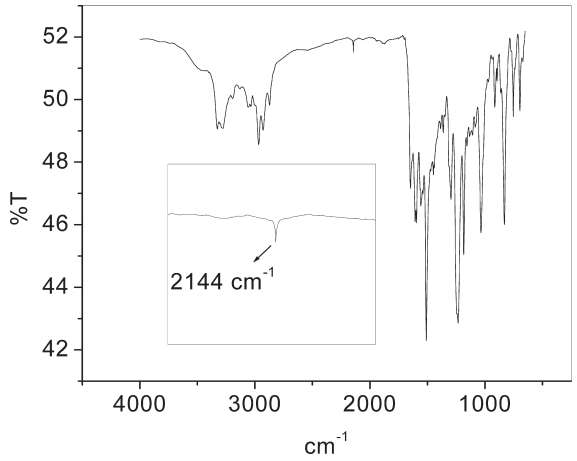

Fig. 12. FTIR spectrum of diphenyl urea and epoxy mixture at ambient condition.

carried out at a lower temperature ($\sim$10–15°C). This was done by cooling the polymer samples sealed in a polythene bag overnight at 0°C and subjecting them to a quick XRD analysis, before attaining the ambient temperature. The sample temperature during analysis is expected to be at a temperature of $\sim$10–15°C. Figure 15 shows XRD of the cooled samples. The X-ray diffraction profiles exhibited two sharp peaks at $2\theta = 20^{\circ}$ and $2\theta = 24^{\circ}$ corresponding to the crystallites of PTMO segments. This shows that the polymer could possess crystallites below the XRD test temperature, which is in agreement with DSC observation. DSC showed a sharp crystalline melting peak for the PTMO-rich system and broad transition for PTMO-starved systems.

3.6 Mechanical Properties

Table 4 compiles the mechanical properties of cured epoxy resins. For the GY series, with the enhancement in epoxy monomer-content, the tensile strength and the initial modulus increase. This increase in mechanical properties is due to the increased crosslinks in the polymer system. Interestingly, the elongation also increases with an increase in

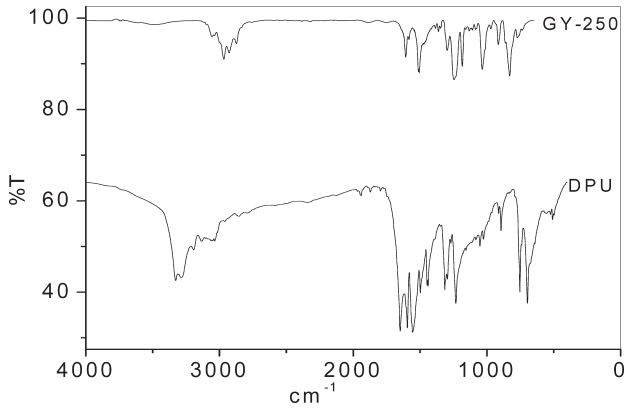

Fig. 13. FTIR spectra of diphenyl urea (DPU) and epoxy resin (GY-250).

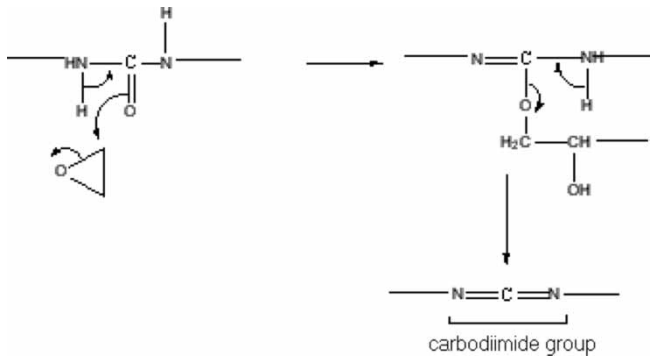

Sch. 2. Likely mechanisms for the formation of a carbodiimide group in the amine-epoxy resin system.

concentration of the epoxy monomer. Highest elongation of 7% was observed for GY-1.1 with a maximum epoxy group-content. Increased elongation of the epoxy monomer-rich system is possibly due to the decrease in concentration of crystalline PTMO in the polymer matrix. EPN and TRI were found to be too brittle to prepare the samples to determine the mechanical properties.

3.7 Dynamic Mechanical Thermal Analysis (DMTA)

Figures 16, 17, and 18 show the DMTA profiles of the cured polymers. The graphs show the variation of storage modulus and tan δ with temperature. For the GY series, storage modulus in the glassy state decreases with an increase in concentration of epoxy monomer as shown in Figure 16. Higher glassy state modulus implies better shape fixity property upon cooling and unloading (18). For GY-0.9, E′ first increases at -48°C and then decreases. This increase in E′ is possibly due to the crystallization of PTMO segments in the system. Figure 17 shows the storage modulus vs. temperature profiles of the three different epoxy systems in the cured state (GY-1.0, EPN-1.0, and TRI-1.0) at 1:1 amine:epoxy equivalent ratio. The storage modulus decreased in the

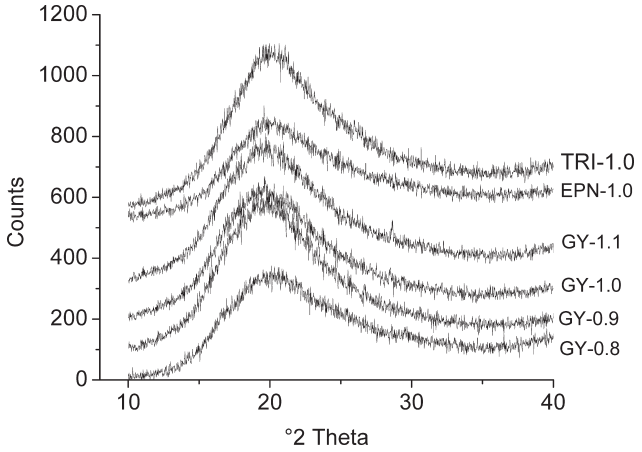

Fig. 14. X-ray diffraction profiles of different polymer systems at ambient temperature (25°C).

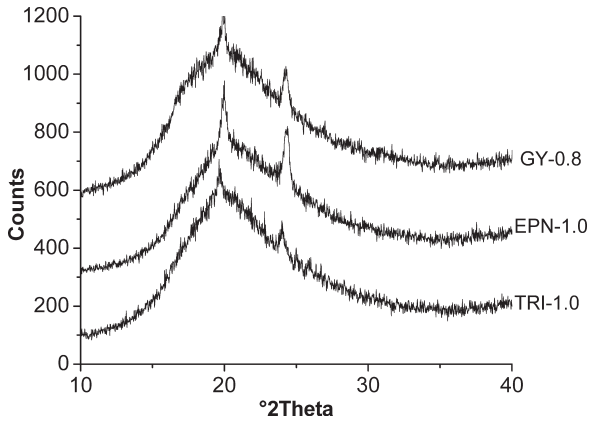

Fig. 15. XRD of cooled samples: GY-0.8, EPN-1.0 and TRI-1.0.

order EPN-1.0 > GY-1.0 > TRI-1.0. Variations of tan δ with temperature for the GY series are shown in Figure 18. With an increase in epoxy monomer concentration, tan δ maximum shifted to a higher temperature region. The temperature corresponding to tan δ maximum was considered as transition temperature (T_{trans}). These transition temperatures were used for fixing the temperature conditions for evaluation of shape memory properties. The T_{trans} values are higher than the melting point observed in the DSC. Similar temperature differences have been observed previously for the shape memory polyurethane system (14). For practical applications, the T_{trans} from DMTA are normally used as the transition temperature.

3.8 Shape Memory Evaluation of Polymers

Shape memory property was evaluated by a bending test at temperatures corresponding to $T_{trans} + 20^{\circ}$C for each system. Table 5 compiles the shape memory characteristics of various polymer systems at the fifth cycle. For the GY series, the sample with maximum PTMO content exhibited 99% shape recovery even after the fifth cycle. With a decrease in PTMO content, the shape recovery characteristics decreased slightly and reached the minimum value of 94% for GY-1.1. EPN-1.0 showed a shape recovery of 85% and TRI-1.0 showed 90% shape recovery. Table 4 includes the shape recovery time at the specified temperatures (T_{Trans}). For the GY series, recovery time decreases with an increase in PTMO content. The sample with 99% shape recovery

Table 4. Mechanical properties of epoxy-based systems (at ambient temperature, 25°C)

Sample reference	Tensile strength (MPa)	Percentage elongation	Initial modulus (MPa)
GY-0.8	2.7	2	100
GY-0.9	21.6	3	410
GY-1.0	24.4	5	560
GY-1.1	39.7	7	605

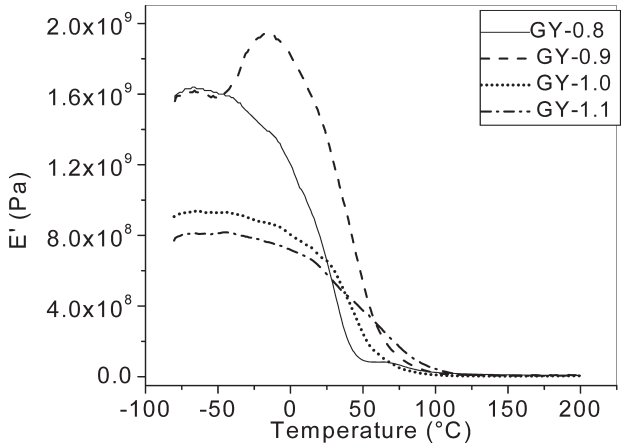

Fig. 16. Storage modulus vs. temperature profiles of cured polymers in the GY series, Heating rate: 5°C/min.

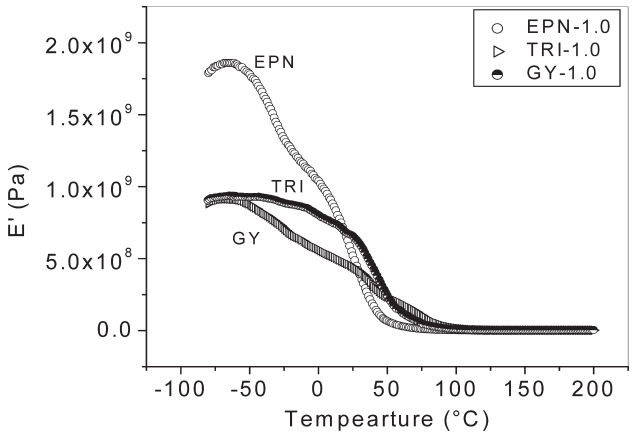

Fig. 17. DMTA of cured resins GY-1.0, EPN-1.0, and TRI-1.0, Heating rate: 5°C/min.

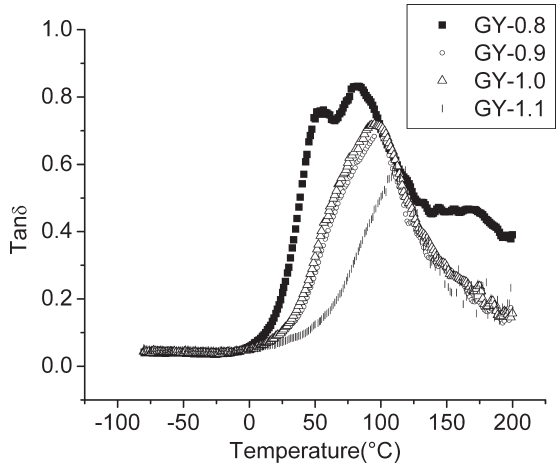

Fig. 18. Tan δ vs. temperature profiles of cured resins in GY series.

Table 5. Shape memory properties of amine-epoxy polymer systems

Sample	% Shape recovery	T_{trans} (DMTA) (°C)	Recovery time (s)
GY-0.8	99	83	12
GY-0.9	98	95	15
GY-1.0	97	96	17
GY-1.1	94	110	30
EPN-1.0	85	77	35
TRI-1.0	90	110	30

required a recovery time of 12 s. For the EPN-1.0, the recovery time is higher than for the GY series. TRI-1.0 recovered in 30 s at par with GY-1.1. Since the shape recovery characteristics increase with PTMO content, it can be concluded that either the crystallization or dipolar interaction of the PTMO segments are responsible for the shape memory characteristics of the polymer system. Normally crystals, glassy states, entanglements or crosslinking structures and strong dipolar interactions are used for fixing the phases for memorizing the original shape (35–37).

4 Conclusions

An epoxy-based shape memory polymer was synthesized by curing epoxy resins with amine telechelic PTMO. Molar ratios of the reactants were varied to get polymers of varying compositions. DSC and rheological analyses were used to monitor the cure reaction of the polymer system. First order kinetics was observed for epoxy: amine reaction from DSC investigation. The isothermal cure prediction from DSC kinetic data matched with the actual cure behavior as observed in rheological analysis. FTIR analysis confirmed the completion of a curing reaction. XRD analysis showed epoxy polymer systems to possess broader crystal dispersion at room temperature and the existence of PTMO crystallites on cooling the resin. Increasing epoxy monomer concentration resulted in progression in T_{trans}, tensile strength and initial modulus. For a given epoxy system, increasing the PTMO concentration is conducive to enhancing the shape recovery characteristics with a marginal penalty in the recovery time. All the epoxy-based systems exhibited more than 85% shape recovery. 99% Shape recovery was observed for GY-0.8 with a maximum PTMO concentration. The system recovered the shape in 12 seconds under the test conditions.

5 Acknowledgments

The authors acknowledge VSSC for granting permission to publish this paper. Thanks are due to IICT, Hyderabad for DMTA analysis, Ms. J.D. Merline, and to the University Grants Commission, New Delhi for a research fellowship.

6 References

1. Liu, G., Ding, X., Cao, Y., Zheng, Z. and Peng, Y. (2005) *Macromol. Rapid Commun.*, **26**, 649.
2. Hu, Z., Zhang, X. and Li, Y. (1995) *Science*, **269**, 525.
3. Osada, Y. and Matsuda, A. (1995) *Nature*, **376**, 219.
4. Lendlien, A. and Langer, R. (2002) *Science*, **296**, 1673.
5. Alteheld, A., Feng, Y., Kelch, S. and Lendlein, A. (2005) *Angew Chem. Int. Ed.*, **44**, 1188.
6. Wang, M. and Zhang, L. (1999) *J. Poly. Sci.: Part B, Poly. Physics.*, **37**, 101.
7. Lin, J.R. and Chen, L.W. (1998) *J. Appl. Poly. Sci.*, **69**, 1575.
8. Li, F. and Richard, C.L. (2002) *J. Appl. Poly. Sci.*, **84**, 1533.
9. Jeong, H.M., Kim, B.K. and Ahn, B.K. *Poly. Int.*, **49**, 1714.
10. Everhart, M.C., Nickerson, D.M. and Hreha, R.D. Source: Proceedings of SPIE - The International Society for Optical Engineering; 6171, Smart Structures and Materials 2006; Industrial and Commercial Applications of Smart Structures Technologies, 2006, p. 61710K.
11. Zhang, C.-S. and Ni, Q.-Q. (2007) *Composite Structures*, **78**, 153.
12. Muhammad, Y.R., Mathias, A., Lars, F. and Bernd, W. (2007) *Materials Science and Engineering A.*, **444**, 227.
13. Merline, J.D., Reghunadhan Nair, C.P., Gouri, C., Shrisudha, T. and Ninan, K.N. (2007) *J. Mater. Sci.*, **42**, 5897.
14. Merline, J.D., Reghunadhan Nair, C.P., Gouri, C., Sadhana, R. and Ninan, K.N. (2007) *Eur. Polym. J.*, **43**, 3629.
15. Takahashi, T., Hayashi, N. and Hayashi, S. (1996) *J. Appl. Polym. Sci.*, **60**, 1061.
16. Kim, B., Lee, K., Lee, S.Y. and Baek, S. (1998) *Polymer.*, **39**, 2803.
17. Ken, G., Martin, L., Liu, Y., Finch, D. and Lake, M. (2002) *Acta Mater.*, **50**, 5115.
18. Kim, B.K., Lee, S.Y. and Xu, M. (1996) *Polymer.*, **37**, 5781.
19. Jeong, H.M., Lee, J.B., Lee, S.Y. and Kim, B.K. (2000) *J. Mater. Sci.*, **35**, 279.
20. Gouher, R., Heinrich, L. and Arno, K. (2006) *Polymer.*, **47**, 4251.
21. Kim, B.K., Shin, Y.J., Cho, S.M. and Jeong, H.M. (2000) *J. Poly. Sci., Part B, Poly, Phys.*, **38**, 2652.
22. Lendlein, A., Annette, M.S., Michiael, S. and Robert, L. (2005) *J. Poly. Sci., Part A, Poly. Chem.*, **43**, 1369.
23. Rabani, G., Luftmann, H. and Kraft, A. (2006) *Polymer.*, **47**, 4251.
24. Beloshenko, V.A., Ya, E.B., Borzenko, A.P. and Varyukhin, V.N. (2002) *Composites, Part A.*, **33**, 1001.
25. Abrahamson, E.R., Lake, M.S. and Munshi, N.A. 43rd Structures, Structural Dynamics and Materials Conference, April 22–25, 2002, Denver, Colorado.
26. Francis, W. and Lake, M. 45th AIAA/ASME/ASCE/AHS/ASC Structures, Structural Dynamics & Materials Confer, Palm Springs, California, April 19–22, 2004; AIAA; 2004, 1821.
27. Lin, J.R. and Chen, L.W. (1999) *J. Appl. Polym. Sci.*, **73**, 1305.
28. Sidney, S. *Quantitative Organic Analysis via Functional Groups*, 3rd Edn; Vol. 558, 1963.
29. Coats, A.W. and Redfern, J.P. (1964) *Nature.*, **201**, 68.
30. Ozawa, T. (1970) *Therm. Anal.*, **2**, 301.
31. Ozawa, T. (1976) *Therm. Anal.*, **9**, 369.
32. Ozawa, T. (1975) *Therm. Anal.*, **7**, 601.
33. Kissinger, H.E. (1956) *J. Res. Nat. Bur. Stand.*, **57**, 217.
34. Bestmann, H.J., Lienert, J. and Mott, L. (1968) *Liebig's Anal. Chem.*, **718**, 24.
35. Lendlein, A. and Steffen, K. (2002) *Angew. Chem. Int. Edn. Engl.*, **41**, 2034.
36. Matsuda, A., Sato, J., Yasunaga, H. and Osada, Y. (1994) *Macromolecules.*, **27**, 7695.
37. Lee, S.H. and Kim, J.W. (2004) *Smart. Mater. Struct.*, **13**, 1345.